



Crown ether-modified polyelectrolytes and their interactions with cations – A QCM study

Sevil Sahin, Emma van Weeren, Han Zuilhof, Louis C.P.M. de Smet*

Laboratory of Organic Chemistry, Wageningen University, Stippeneng 4, Wageningen 6708 WE, the Netherlands

ARTICLE INFO

Keywords:

Polyelectrolyte multilayers
Crown ether
Bio-based polymer
Pectin
Ion selectivity

ABSTRACT

In this study, the build-up of polyelectrolyte multilayers (PEMs) containing 15-crown-5 (CE) groups and their interactions with various cations were studied by using quartz crystal microbalance with dissipation monitoring (QCM-D). First, poly(allylamine hydrochloride) (PAH) was modified with 4'-carboxybenzo-CE via carbodiimide chemistry. CE was chosen as its complexes with Na^+ and K^+ are reported to be more stable compared to those with other cations. The resulting functionalized polyelectrolyte (PAHCE) and poly(4-styrene sulfonic acid) (PSS) were used in the layer-by-layer build-up of a multilayer onto gold-coated quartz resonators, enabling their characterization with QCM-D. Compared to $(\text{PAH}/\text{PSS})_4$, $(\text{PAHCE}/\text{PSS})_4$ resulted in slightly thicker layers based on Voigt (65 ± 5 vs. 57 ± 3 nm) and Sauerbrey (45 ± 2 vs. 38 ± 3 nm) modelling of the QCM-D data. The same trend was found for the optical, dry thickness, as obtained with ellipsometry (15 ± 0.3 vs. 13 ± 1 nm). Next, the QCM-D characteristics of these PEMs were monitored *in situ* when exposed to various aqueous salt solutions (LiCl, NaCl, KCl, CsCl, RbCl, and MgCl_2). Starting from Cs^+ , the frequency change of the $(\text{PAHCE}/\text{PSS})_4$ system upon changing to K^+ and Na^+ solutions was found to be ≈ 3 times larger than for $(\text{PAH}/\text{PSS})_4$. With a polycation (PAHCE) as the outermost PEM layer, the salt-exchange behavior was less visible due to increased charge rejection of cations. Therefore, we also modified a bio-based polyanion, pectin with 4'-aminobenzo-CE and built $(\text{PAH}/\text{pectinCE})_4$. Also in this case, the addition of CE increased the PEM layer thickness compared to $(\text{PAH}/\text{pectin})_4$, both in a wet state (Sauerbrey modelling, 447 ± 19 vs. 314 ± 17 nm) and when dry (115 ± 4 vs. 66 ± 3 nm). Again, we observed the largest QCM-D responses for K^+ and Na^+ solutions (≈ 6 and 12 times larger, respectively) compared to $(\text{PAH}/\text{pectin})_4$. The effect of CE is more prominent in pectin-based PEMs due their relatively higher thickness. Given the large toolbox of available polyelectrolytes and ionophores, we anticipate that functionalized PEMs can facilitate the further development of ion separation applications.

1. Introduction

Selectivity is crucial for applications that involve the detection and separation of ions, including in clinical chemistry [1], environmental monitoring [2], and water treatment [3–6]. For instance, K^+ and Na^+ selectivity is important for a rapid and reliable detection of these ions, which both play a regulating role in the cellular electrolyte metabolism [7], while K^+ over Na^+ selectivity is important for greenhouse applications, as it assists the recycling of irrigation water [4]. Other examples from the field of water treatment include the reduction of water hardness (divalent over monovalent selectivity) [3,5], and the recovery of nutrients, such as phosphate [5,6,8,9], and valuable metals such as lithium [10,11]. Similarly, levels of arsenic, lead, and mercury are monitored to check heavy metal contamination in the environment and

blood samples [12].

One interesting and attractive way to tune ion selectivity is to introduce polyelectrolyte multilayers (PEMs) [5,6,8,10,11,13–16]. PEMs are composed of alternating layers of oppositely charged polymers and can control the physicochemical properties of various surfaces, including those of membranes and electrodes [17–21]. As such, PEMs provide a versatile and facile way to tune separation processes of various species like gases, solvents and ions [22,23]. Moreover, the selectivity of PEMs strongly depends on structural features like the molecular weight and/or charge density of the constituting polyelectrolytes [19,24–26], the number of layers in the PEM, as well as experimental conditions, including the ionic strength [27–29], the type of supporting electrolyte [30–33] and the pH [34–37] of the solution in which the PEM is prepared or in contact with.

* Corresponding author.

E-mail address: louis.desmet@wur.nl (L.C.P.M. de Smet).

<https://doi.org/10.1016/j.apsadv.2022.100271>

Received 23 March 2022; Received in revised form 18 June 2022; Accepted 3 July 2022

Available online 7 August 2022

2666-5239/© 2022 The Authors. Published by Elsevier B.V. This is an open access article under the CC BY-NC-ND license (<http://creativecommons.org/licenses/by-nc-nd/4.0/>).

The ion-separation properties of PEMs mostly rely on their charge- and size-dependent rejection mechanisms towards a certain (type of) ion [3,22,23,38]. Interestingly, the ion-selective behavior of PEMs can be further tuned via the incorporation of ionophores. Typically one of the polyelectrolytes is replaced by an ionophore during layer build-up, or the ionophore is trapped within the PEM [39–41]. For example, Toutianoush et al. combined various negatively charged calixarene derivatives with poly(vinyl amine) to build calixarene-functionalized PEMs, which demonstrated ion-selective properties towards monovalent, divalent, or trivalent cations based on the ring size of the calixarene ring [39]. However, the lack of covalent bonds between the macromolecular polyelectrolytes and low-molecular-weight ionophores makes such systems limited in stability due to the problem of leaching of the ionophore to the environment. Alternatively, ionophores are covalently attached to the polyelectrolyte backbone [9,10]. For instance, Cao et al. chemically attached guanidinium moieties to a polycation, to yield a functional macromolecule that was found to be useful in building PEMs that showed increased interactions with phosphate ions [8,9,42].

Given the importance of PEMs in alkali metal ion recognition processes, including those relevant for ion sensors [1,4,40,41,43–47] and pressure-driven ion separations [39,48,49], we now covalently attached a crown ether to polyelectrolytes and incorporated these in PEMs for ion selectivity.

In order to study the structure of (functionalized) PEMs and their interaction with different ions, quartz crystal microbalance with dissipation monitoring (QCM-D) is a widely used technique [9,50–53]. In short, QCM-D makes use of a resonating gold-coated, piezo-active sensor onto which PEM layers can be built [54,55]. The resonance frequency is monitored online and frequency changes are proportional to the changes in mass, as shown by Eq. (1): [56]

$$\Delta m = \frac{-C \times \Delta f_n}{n} \quad (1)$$

where Δm ($\text{ng} \cdot \text{cm}^{-2}$) is the areal mass density of the adsorbed film, C ($1.77 \text{ ng} \cdot \text{cm}^{-2} \cdot \text{Hz}^{-1}$) is the mass-sensitivity constant, Δf_n (Hz) is the frequency shift and n is the harmonic number (3, 5, 7, 9, 11). The thickness of the films is determined either using the Sauerbrey model, which is suitable for rigid layers, or using a viscoelastic model that is mainly used for soft PEM coatings [50,51,57]. Furthermore, the dissipation mode of QCM-D enables one to obtain information on the viscoelastic properties of the layers.

In this study, we aim to extend the scope of ion-selective PEM coatings by attaching crown ether units as ionophore to two polyelectrolytes, and to better understand the interactions between the functionalized PEMs – as well as their non-functionalized equivalents – and various cations. Although the effects of different anions on the PEM structure have been studied previously via QCM-D [28,33,58–61], a comparable, comprehensive study with alkali (earth) metal cations has not been reported yet. Also, the cation preference of an ionophore-containing PEM has not been studied yet with QCM-D. In addition, apart from an interesting series of adsorption selectivity studies on crown ether-functionalized chitosan [62–68], the number of studies on crown ether-functionalized, bio-based polyelectrolytes for ion studies is limited [62]. Moreover, in those studies atomic adsorption spectrophotometry was exclusively used to analyze the metal concentrations in supernatant solutions of centrifuged polyelectrolyte-salt solutions. While this was useful in terms of adsorption selectivity at the single polyelectrolyte level, the use of PEMs also enables the use of surface-related analytical techniques. In this study, we covalently attached 15-crown-5 (CE) to both poly(allylamine hydrochloride) (PAH) and pectin, to obtain different PEMs that are decorated with ionophore groups. Pectin was the natural polyelectrolyte of choice since it can be obtained from citrus peel, making it an affordable and biodegradable polyanion, while PAH is widely used polycation to build PEMs. CE was chosen as its complexes with Na^+ and K^+ are reported to be more stable

compared to those with other cations [69–72]. The interactions between various cations and CE-containing PEMs and their non-functionalized equivalents as well as the effect of CE modification on PEM properties were studied by a real-time gravimetric method, QCM-D.

2. Materials and methods

2.1. Materials

Poly(allylamine hydrochloride) (PAH, $M_w \approx 450,000$ Da), poly(sodium 4-styrenesulfonic acid) solution (PSS, $M_w \approx 75,000$, 18 wt. % in H_2O), pectin (from citrus peel, galacturonic acid $\geq 74.0\%$ (dried basis)), 4'-carboxybenzo-15-crown-5 (>98%), 4'-aminobenzo-15-crown-5 (97%), *N*-hydroxysuccinimide (NHS, 98%), *N*-(3-dimethylamino-propyl)-*N'*-ethylcarbodiimide hydrochloride (EDC, >98%), lithium chloride (BioXtra, $\geq 99.0\%$), sodium chloride (NaCl, $\geq 99\%$), potassium chloride (BioXtra, $\geq 99.0\%$), rubidium chloride (ReagentPlus®, $\geq 99.0\%$ (metals basis)), cesium chloride (ReagentPlus®, 99.9%), anhydrous magnesium chloride (MgCl_2 , $\geq 98\%$), sodium dodecyl sulfate (ACS reagent, $\geq 99.0\%$), 3-(trimethylsilyl)propionic-2,2,3,3-d₄ acid sodium salt (TSP-D4), and Hellmanex™ III (cleaning concentrate) were purchased from Sigma Aldrich. Hydrochloric acid (36.5 – 28.0% NF grade) was purchased from VWR International. All chemicals were used as received without further purification. The inorganic salts were kept in a vacuum oven overnight prior to use. Dialysis membrane cellulose tubing (with a cut-off ≈ 14 kDa) was bought from Sigma Aldrich. Milli-Q water (18.2 $\text{M}\Omega \cdot \text{cm}$, Milli-Q Integral 3 system, Millipore) was used to prepare salt and polyelectrolyte solutions. Gold-coated quartz resonators (AT-cut, QSense 301, < 1 nm RMS, 100 nm Au) with a fundamental frequency (f_0) of 5 MHz were purchased from Biolin Scientific, Sweden.

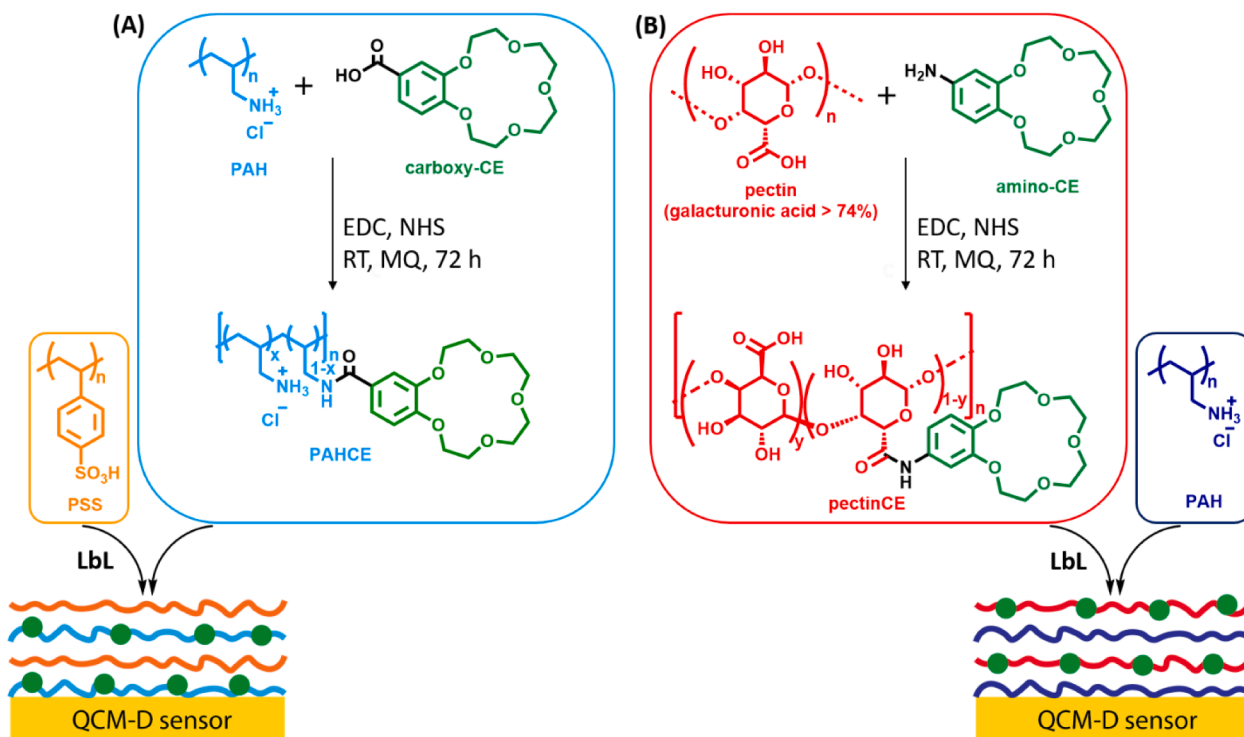
2.2. Methods

2.2.1. Synthesis and purification of the crown-ether functionalized polyelectrolytes

EDC-NHS carbodiimide-assisted coupling reactions were used to synthesize crown-ether containing polyelectrolytes. The protocol was adapted from the work of Cao et al. [9].

A series of PAH derivatives with different degrees of substitution were synthesized by changing the molar feed ratio of the monomeric allylamine hydrochloride and 4'-carboxybenzo-15-crown-5 (carboxy-CE). The synthesized products were abbreviated as PAHCE #1, PAHCE #2, and PAHCE #3 for the feed ratios of 10:1, 10:2, and 10:3, respectively. Amino groups of the PAH reacted with the carboxylic acid groups of the carboxy-CE to yield a conjugate of the two molecules joined by a stable amide bond (Scheme 1A). Briefly, for the 10:2 ratio case, PAH (0.2 g, 2.140 mmol, 1 equiv.) and carboxy-CE (0.134 g, 0.428 mmol, 0.2 equiv.) were dissolved 30 mL of Milli-Q water. Followed by the addition of 1-ethyl-3-(3-dimethylaminopropyl)carbodiimide (0.984 g, 5.136 mmol, 2.4 equiv.) and *N*-hydroxysuccinimide (0.492 g, 4.28 mmol, 2 equiv.). The reaction mixture was stirred for 72 h at room temperature. The mixture was afterwards transferred to a dialysis tube (cut-off 14 kDa), which was then kept in ample Milli-Q water for 48 h. The water was refreshed every 12 h, and at the end of the dialysis the retained mixture was freeze dried. In the rest of the study, PAHCE #2 derivative was used unless otherwise stated.

Similarly, pectin was functionalized with 15-crown-5 (Scheme 1B). The carboxylic acid groups (of which the pK_A is generally believed to be in the range between pH 3.5 and pH 4.5) of pectin do not only make it a polyanion, but can also be used to covalently attach an amino-CE. In more detail, pectin was functionalized with 4'-aminobenzo-15-crown-5 (amino-CE) by using a 10:2 feed ratio. Pectin (0.1 g, 0.497 mmol, 1 equiv.) and amino-CE (0.028 g, 0.099 mmol, 0.2 equiv.) were dissolved in 20 mL of Milli-Q water, to which was subsequently added 1-ethyl-3-(3-dimethylaminopropyl)carbodiimide (0.229 g, 1.193 mmol, 2.4 equiv.) and *N*-hydroxysuccinimide (0.114 g, 0.994 mmol, 2 equiv.). The



Scheme 1. Reaction schemes for the synthesis of (A) PAHCE and (B) pectinCE and schematic representations of the PEM-coated QCM sensors.

reaction mixture was stirred for 72 h at room temperature. The mixture was afterwards transferred to a dialysis tube (cut-off 14 kDa) and kept in ample Milli-Q water for 48 h. The water was refreshed every 12 h, and at the end of the dialysis the mixture was freeze dried.

Since the molecular weight of the functionalized polyelectrolytes was not exactly known, yields were calculated by dividing the mass of the product obtained after the purification by the sum of the masses of the reactants (either PAH and carboxy-CE or pectin and amino-CE), as described in the literature [9].

2.2.2. Characterization of PAHCE and pectinCE

The structures of the products were characterized by nuclear magnetic resonance (NMR) spectroscopy (Bruker AVANCE, 400 MHz for ^1H and 101 MHz for ^{13}C with deuterated water (D_2O) as solvent). In addition to one-dimensional NMR experiments, two-dimensional NMR experiments, correlation spectroscopy (COSY), heteronuclear single quantum coherence (HSQC), and heteronuclear multiple bond correlation (HMBC), were conducted for PAHCE. Additionally, diffusion-ordered spectroscopy (DOSY) was used to confirm the covalent bonds between the CE moieties and PAH backbone. TSP- d_4 was used as an internal standard when acquiring the ^1H -NMR spectrum of pectinCE by dissolving 14.1 mg of pectinCE and 0.65 mg of TSP- d_4 in 1 mL of D_2O . The spectra were processed with MasterNova 14.1.0.

Fourier-transform infrared (FT-IR) spectra were recorded with a Bruker Tensor 27 spectrometer equipped with a platinum attenuated total reflection (ATR) accessory. The samples were placed on the crystal of the ATR accessory as powder. Each spectrum was acquired with 64 scans with a resolution of 4 cm^{-1} .

2.2.3. Preparation of polyelectrolyte and salt solutions

Salt solutions (0.15 M) were prepared by dissolving the appropriate amount of salt in Milli-Q water. The pH of these solutions was adjusted to 5.0 (using a pH meter, Innolab, WTW series) by adding drops of a diluted HCl solution. Polyelectrolyte solutions were prepared by dissolving 25 mg of the polyelectrolyte in 50 mL of CsCl solution (0.15 M, at pH 5.0).

2.2.4. Multilayer build-up

The experiments were performed by using gold-coated quartz sensors in a QCM-D set-up (Q-Sense E4, Biolin Scientific, Sweden) at 18°C . Prior to the experiments, the sensors were dipped in a 2% sodium dodecyl sulfate solution for 30 min, and rinsed excessively with Milli-Q water. After rinsing, they were dried with a flow of nitrogen and treated with UV-ozone cleaner (Procleaner UV.PC.220, Bioforce Nanosciences) for 20 min.

All polyelectrolyte and salt solutions were bubbled with nitrogen for 15 min in order to reduce the concentration of dissolved oxygen that may cause an unstable baseline. The flow rate of solutions was $50\ \mu\text{L}/\text{min}$ in all experiments.

Before each experiment, a CsCl solution (0.15 M, at pH 5.0) was pumped through the QCM-D cells via a peristaltic pump (Ismatec, high precision multichannel dispenser) for 30 min to have a stable baseline. Afterwards, the resonance frequency and dissipation values obtained with CsCl were recorded as baseline and the deposition of polyelectrolytes started by switching to the appropriate solution. The real-time build-up of PEMs started with a polycation for each experiment. The PEMs abbreviated as (PAH/PSS) $_n$, (PAHCE/PSS) $_n$, (PAH/pectin) $_n$, and (PAH/pectinCE) $_n$, where n indicates the number of bilayers. Alternating layers of polycation and polyanion were deposited on the gold sensors by alternate pumping of each solution for a minimum of 10 min to build the PEMs. After the build-up, a CsCl solution was pumped to the PEM to remove any weakly attached polyelectrolytes. Then, salt-exchange experiments were performed by using the PEM-coated sensors. Note that the term salt- or ion-exchange [9,58], or alternatively specific ion effect [61], is regularly used in studies where coatings are exposed to different salt conditions.

Frequency (Δf) and dissipation shifts (ΔD) were acquired at the 3rd (15 MHz), 5th (25 MHz), 7th (35 MHz), 9th (45 MHz), and 11th (55 MHz) harmonic overtones. The 3rd overtone was chosen for the comparison of various experiments as it is one of the most suitable harmonics to reflect the surface character of the film [9,34,35]. The data was recorded with QSoft (version 2.8.0.913, Analyzer) and analyzed with DFind (version 1.2.7) software. The mass of the assembled PEMs was calculated by

using the Sauerbrey equation (Eq. (1)), and the (wet) PEM thicknesses were calculated based on Sauerbrey modelling in DFind. Eq. (1) shows that decrease of frequency is associated with increase in mass, therefore a higher thickness value. As Sauerbrey modelling is for rigid films, the wet thicknesses of the films were also estimated via Voigt modelling in DFind. In Voigt modelling, the density of the default bulk liquid water (20 °C) was chosen as 998 g/L and the densities for the default layer materials were chosen as 1020 g/L (PAH), 1050 g/L (PSS), and 1300 g/L (pectin).

2.2.5. Spectroscopic ellipsometry analyses

The optical (dry) thickness of the PEM coatings was measured after freshly-coated sensors were rinsed with Milli-Q water and dried with a gentle flow of nitrogen. The data were obtained by using an Accurion Nanofilm_ep4 imaging ellipsometer in air at room temperature. The wavelength range of the light was $\lambda = 400.6\text{--}761.3$ nm at an angle of incidence of 50°. The data were fitted with EP4 software using a multilayer model and a refractive index of 1.397 for gold.

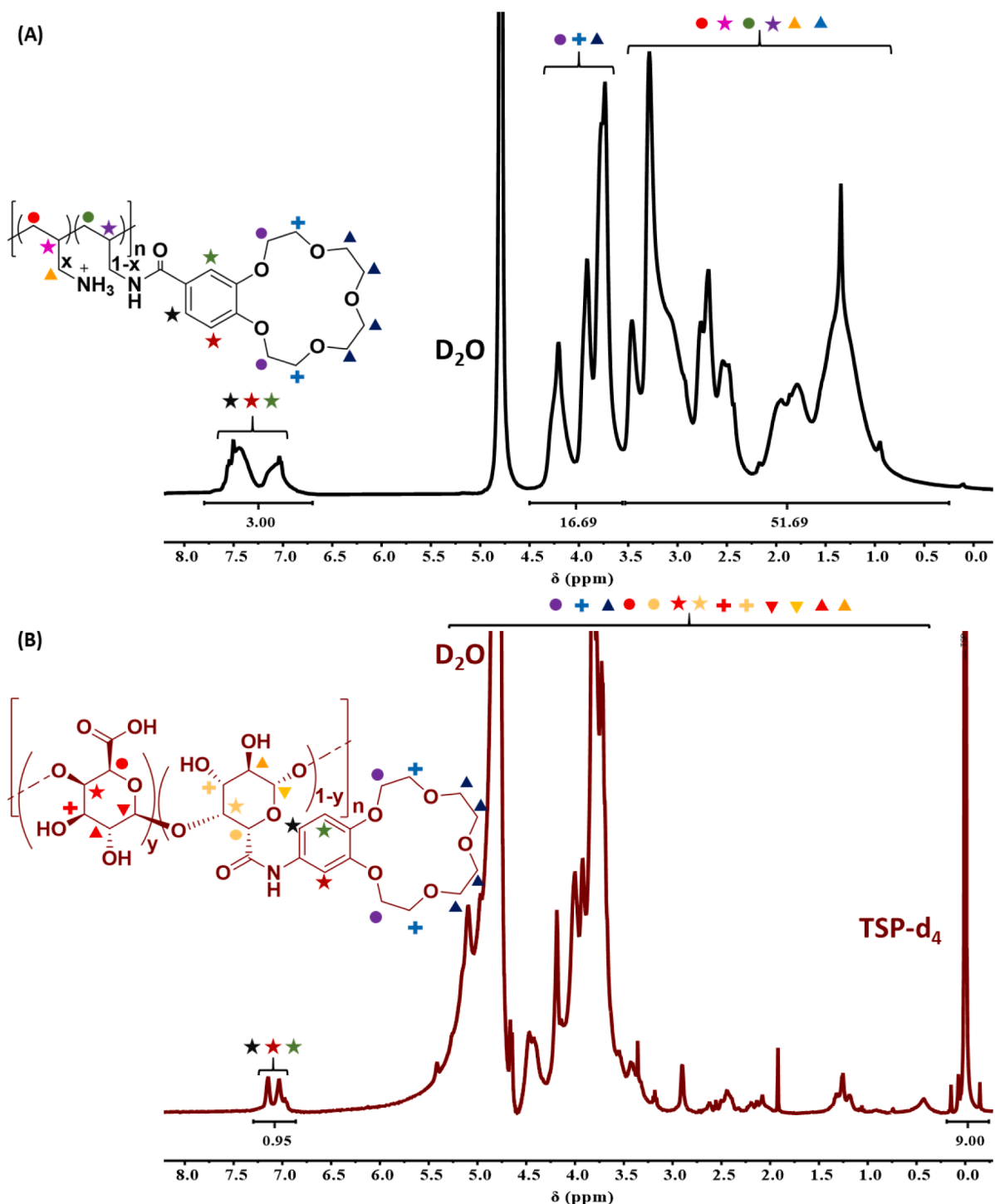


Fig. 1. ¹H-NMR spectra of (A) PAHCE #2 (400 MHz, D₂O) δ 7.69 – 6.69 (m, 3H), 4.50 – 3.56 (m, 17H), 3.53 – 0.25 (m, 52H), and (B) pectinCE with TSP-d₄ as an internal standard.

2.2.6. Salt-exchange experiments with QCM-D

After the aforementioned PEMs were built, a CsCl solution (0.15 M, pH 5.0) was flushed through the QCM-D cell for at least 30 min to get a stable baseline. Once achieved, various salt solutions (e.g. LiCl, NaCl, KCl, RbCl, MgCl₂, etc.) were pumped to the QCM-D cells one by one. Each salt solution was pumped through the QCM-D cell for at least 30 min. Finally, the salt solutions were replaced by a CsCl (0.15 M, pH 5.0) solution to reach the baseline.

After the experiments, 50 mL of 1% (v/v) Hellmanex III solution was run through the QCM-D cell at 40 °C. Then, the system was rinsed with at least 50 mL of Milli-Q water, before drying it upon air. All PEM build-up and salt-exchange experiments were repeated at least three times, and the reported values result from averaging the resulting data.

3. Results and discussion

3.1. Synthesis and characterization of PAHCE and PectinCE

Crown ether-functionalized PAH derivatives (PAHCE #1, PAHCE #2, and PAHCE #3) were synthesized via a carbodiimide-assisted coupling reaction as shown in Scheme 1A by using different molar feed ratios of the polymer and CE. The combination of bands in the aromatic and aliphatic region of the ¹H-NMR spectrum of PAHCE #2 (Fig. 1A) does not only show that the attachment was successful; it can also be used for a quantitative analysis. In more detail, the bands in the 3.53-0.25 ppm region are attributed to the protons in the PAH backbone (–CH₂–CH–) and the methylene protons in the side chain (–CH₂–NH₂ / CH₂–NHR). The chemical shift of these aliphatic signals was confirmed by ¹H-NMR and HSQC spectra of the unmodified PAH (Figs. S1 and S2). The signals at 7.69 – 6.69 ppm and 4.50 – 3.56 ppm can be attributed to three protons of the aromatic moiety in the CE and the aliphatic CH₂O signals of the crown ether, respectively. The degree of modification was calculated by comparing the integration of the aromatic protons of the crown ether and the aliphatic protons of PAH. Based on this calculation, the degree of substitution for PAHCE #2, for which the feed ratio was 20%, was found to be 9±1%, which is comparable to those of other functionalized polyelectrolytes [9,20]. Additionally, also ¹³C NMR, DOSY, and COSY spectra confirmed the attachment of CE units to the polymer backbone (Figs. S8–10). After the purification step, PAHCE was obtained as a yellow solid with a yield of 91% ± 4. Similarly, the degree of modification for PAHCE #1 and PAHCE #3 was found to be 5% and 14% (Figs. S5 and S6).

Pectin was also successfully functionalized with CE as confirmed with ¹H-NMR (Fig. 1B). After purification, pectinCE was obtained as white solid with a yield of 75% ± 9. The degree of modification was calculated based on the known concentration of pectinCE and TSP-d₄ dissolved in D₂O and the observed integral values of the aromatic protons and TSP-d₄ signal. This showed that the w/w% of CE units in the pectinCE is 2.3 ± 0.3, meaning ≈1.7 mol% CE in pectinCE. Although, the degree of functionalization is relatively lower than the one of PAHCE (9 ± 1%), this can partly be explained by the nature of pectin. It is noted that this percentage is with respect to all monomer units, i.e., those with free carboxylic acid moieties (>74%) and those with the non-reactive methyl esters (<26%). Therefore not all monomers of pectin are available for functionalization, unlike PAH.

All four polymers, i.e. PAH, PAHCE, pectin, and pectinCE, were also analyzed by FT-IR (Fig. 2) and here we describe the main differences upon functionalization. In case of PAHCE (Fig. 2A) the characteristic amide C=O stretching peak at 1632 cm⁻¹ and in-plane N–H bending peak at 1527 cm⁻¹ confirm the presence of the C=O amide bond between PAH and CE moieties [9]. Also, C–H stretching bands of unsaturated (sp²) carbon bonds (3100–3000 cm⁻¹) correspond the aromatic ring of the crown ether moieties. Lastly, although difficult to assign with certainty as it is in the middle of the fingerprint region, the strong signal at 1127 cm⁻¹ can likely be attributed to C–O stretching vibrations, and thus also point to the presence of crown ether moieties [73]

The differences between the FT-IR spectra of pectin and pectinCE are less prominent. In case of pectin, the signals at 1600 cm⁻¹ and 1735 cm⁻¹ correspond to the vibrations of the acid and ester carbonyls, respectively [74]. Although in case of pectinCE an additional amide-based carbonyl signal would be expected, it is difficult to observe such a signal due to the overlapping signals in the carbonyl region. Instead, in this region, while the other two carbonyl-related signals in the IR spectra of pectin and pectinCE appear at the same position, one of the bands shifts from 1735 cm⁻¹ to 1743 cm⁻¹ upon the functionalization, suggesting a change in the structure after additional of CE groups.

To further analyze the structure of pectinCE, X-ray photoelectron spectroscopy was used in addition to ¹H-NMR and FTIR.

Fig. S14 shows the wide-scan XPS spectra of pectin (Fig. S14A) and pectinCE (Fig. S14B), which are coated on gold substrates. Typically, a wide-scan XPS spectrum is associated with a table that provides the elemental composition and the percentage of those elements as well as their binding energies. In case of pectin (Fig. S14A), only C and O peaks are present in the spectrum as expected based on its structure. However,

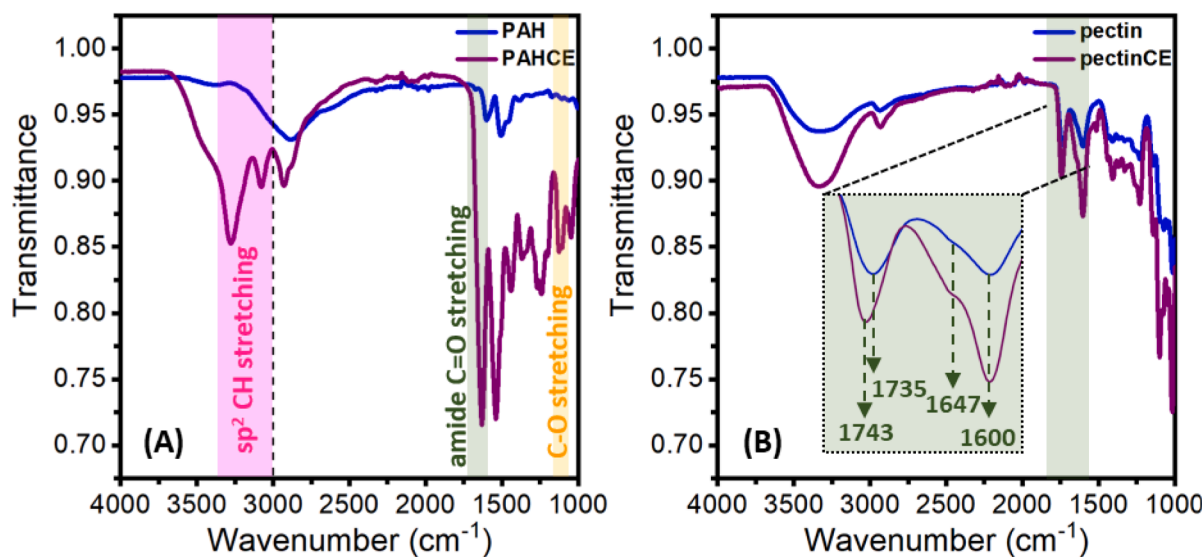


Fig. 2. FT-IR spectra of (A) PAH (blue) and PAHCE (purple) (B) pectin (blue) and pectinCE (purple). The bands that appear upon the functionalization are designated by the boxes and related text labels.

the XPS spectrum of pectinCE (Fig. S14B) shows $\sim 3\%$ of N, indicating the presence of crown ether units linked via amide bonds. Since (i) the peak integration is not accurate for such small peaks and (ii) it is hard to determine the exact % C due to the carbon contaminants in air, it is not possible to obtain accurate values for the degree of functionalization based on XPS spectra. However, qualitatively XPS shows that the synthesis of pectinCE was successful, which is in line with the $^1\text{H-NMR}$ data.

In conclusion, both PAHCE and pectinCE were synthesized successfully and their structures were characterized with various spectroscopic techniques. After characterization of PAHCE and pectinCE, the build-up of PEMs on gold-coated QCM sensors was studied with QCM-D.

3.2. PEM build-up of $(\text{PAHCE}/\text{PSS})_4$

First, a well-studied PAH/PSS PEM [19,51,75] was chosen to see the effect of CE moieties in the layer build-up. In order to compare the layer properties, an equal number of layers (four bilayers) was coated for all types of PEMs. Fig. 3 shows a representative real-time change in frequency and dissipation response for the 3rd, 5th, and 7th harmonics of $(\text{PAHCE}/\text{PSS})_4$ and $(\text{PAH}/\text{PSS})_4$. CsCl was chosen as the supporting electrolyte for the PE solutions as the relatively large Cs^+ ions have less interaction with CE derivatives compared to the smaller alkali metal

ions [69,76]. Therefore, each build-up (and intermediate washing step) was started by flushing a 0.15 M CsCl solution over a bare QCM sensor until a stable base line was observed. Each time that a polyelectrolyte solution was flushed through the QCM-D cell in an alternating fashion in terms of polycation and polyanion, the frequency decreased with a concomitant increase in the dissipation, resulting in cumulative plots that are typical for the build-up of PEMs [9,61,77,78]. Table 1 provides an overview of the averaged QCM data for the various samples. The overall averaged frequency shift for $(\text{PAHCE}/\text{PSS})_4$ was found to be higher than the one of $(\text{PAH}/\text{PSS})_4$ (257 ± 10 Hz vs. 218 ± 14 Hz), while the average change in the dissipation was comparable (41 ± 4 ppm and 43 ± 5 ppm, respectively). These results indicate the CE units contribute to the adsorbed mass, but that this has no effect on the viscoelastic properties of the PEM.

Next, based on the frequency and dissipation shifts the thickness of the PEMs was calculated by using the Sauerbrey and Voigt models (Table 1, top entries). For the PAH/PSS system the use of PAHCE results in a larger (wet) thickness. Although the Sauerbrey model gives an approximate thickness based on frequency change [79], the Voigt model gives a more realistic thickness value for viscous and hydrated layers [50,55,57]. For such systems, harmonics are well separated from each other and spread as shown in Fig. 3. After the QCM-D experiments, the

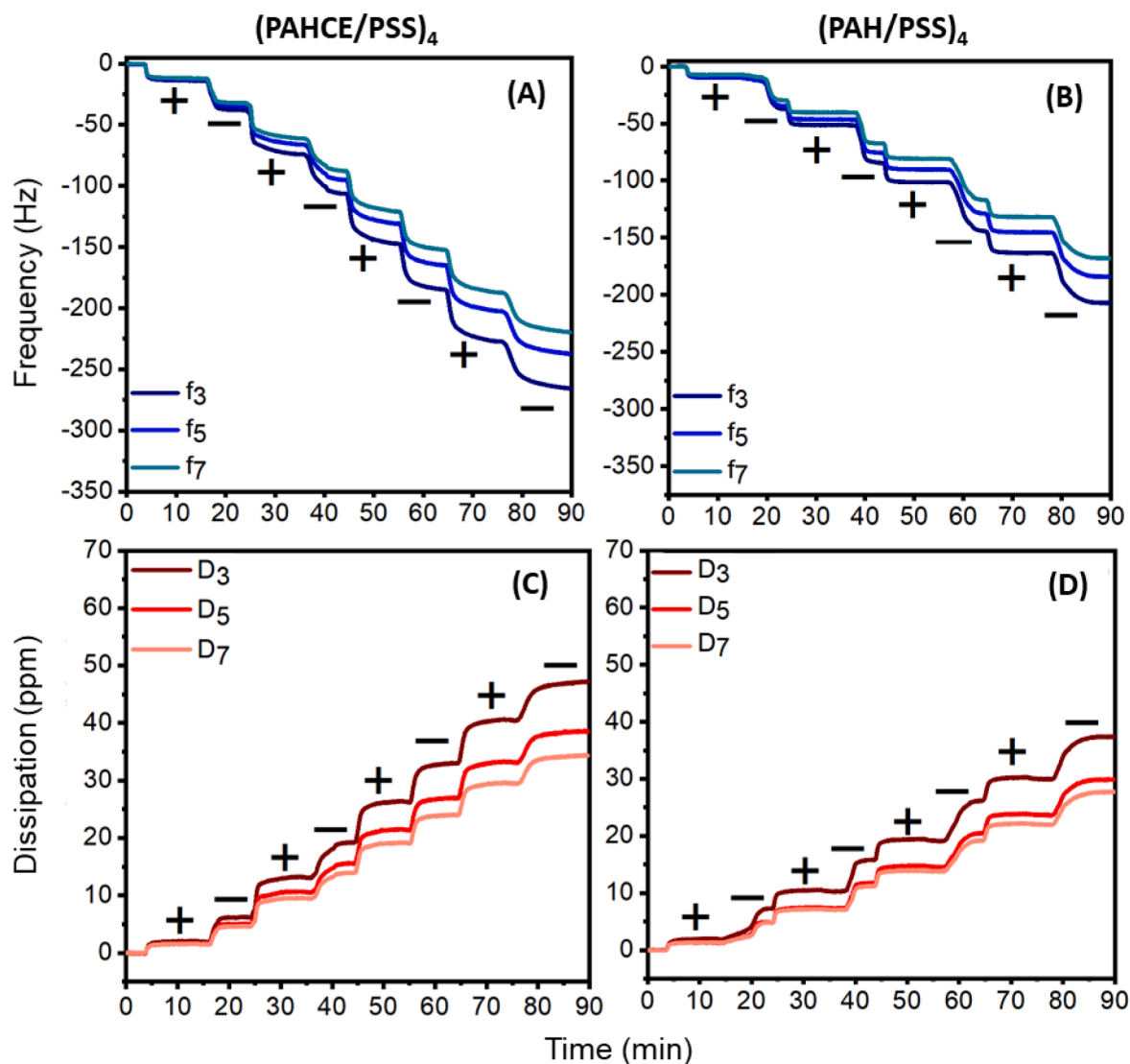


Fig. 3. Real-time QCM-D data showing representative changes in the frequency (A and B) and dissipation (C and D) for the 3rd, 5th, and 7th overtones of the build-up of $(\text{PAHCE}/\text{PSS})_4$ (A and C) and $(\text{PAH}/\text{PSS})_4$ (B and D) in 0.15 M CsCl. The plus and minus signs represent the polycation and polyanion in the PEMs, respectively.

Table 1

The total change in frequency and dissipation for (PAH(CE)/PSS)₄, (PAHCE/PSS)_{3,5}, and (PAH/pectin(CE))₄ multilayers and the modelled (Sauerbrey and Voigt) and the optical thickness values of the PEMs. Each value is the average of three independent experiments.

Type of PEM	Δf_3 (Hz)	ΔD_3 (ppm)	Sauerbrey thickness (nm)	Voigt thickness (nm)	Optical thickness (nm)
(PAH/PSS) ₄	-218 ± 14	41 ± 4	38 ± 3	57 ± 3	13 ± 1
(PAHCE/PSS) ₄	-257 ± 10	43 ± 5	45 ± 2	65 ± 5	15 ± 0.3
(PAHCE/PSS) _{3,5}	-235 ± 8	37 ± 1	41 ± 1	60 ± 4	15 ± 2
(PAH/pectin) ₄	-1757 ± 93	303 ± 44	314 ± 17	- ^a	66 ± 3
(PAH/pectinCE) ₄	-2497 ± 105	455 ± 56	447 ± 19	- ^a	115 ± 4

^a Data did not fit the Voigt modelling. Please see section 3.3 for further explanation and discussion.

QCM sensors were rinsed with MQ water and dried with a flow of nitrogen to measure their optical thickness values via ellipsometry. As expected, given their air-dried state, the optical thickness of (PAHCE/PSS)₄ and (PAH/PSS)₄ PEMs are smaller than the modelled wet thickness values. Although less pronounced, the CE does result in a larger optical thickness. The obtained wet and dry thickness values for (PAH/PSS)₄ were found to be in line with values reported in literature [9,78,80].

3.3. PEM build-up of (PAH/pectin(CE))₄ with QCM-D

Next, as an alternative to PAH/PSS PEM, which is fully of fossil-based origin, we studied the use of a natural polyanion, pectin. PAH/pectin and PAH/pectinCE PEMs were built on the QCM sensors in a similar fashion as the PAH(CE)/PSS PEMs. Fig. 4 shows the real-time change in the frequency and dissipation responses of the 3rd, 5th, and 7th harmonics, confirming the successful the build-up of (PAH/pectinCE)₄ and (PAH/pectin)₄ PEMs. Compared to PAH(CE)/PSS PEMs, PAH/pectin(CE) PEMs have higher frequency and dissipation shifts. From these data it becomes clear that the differences in frequency and dissipation are

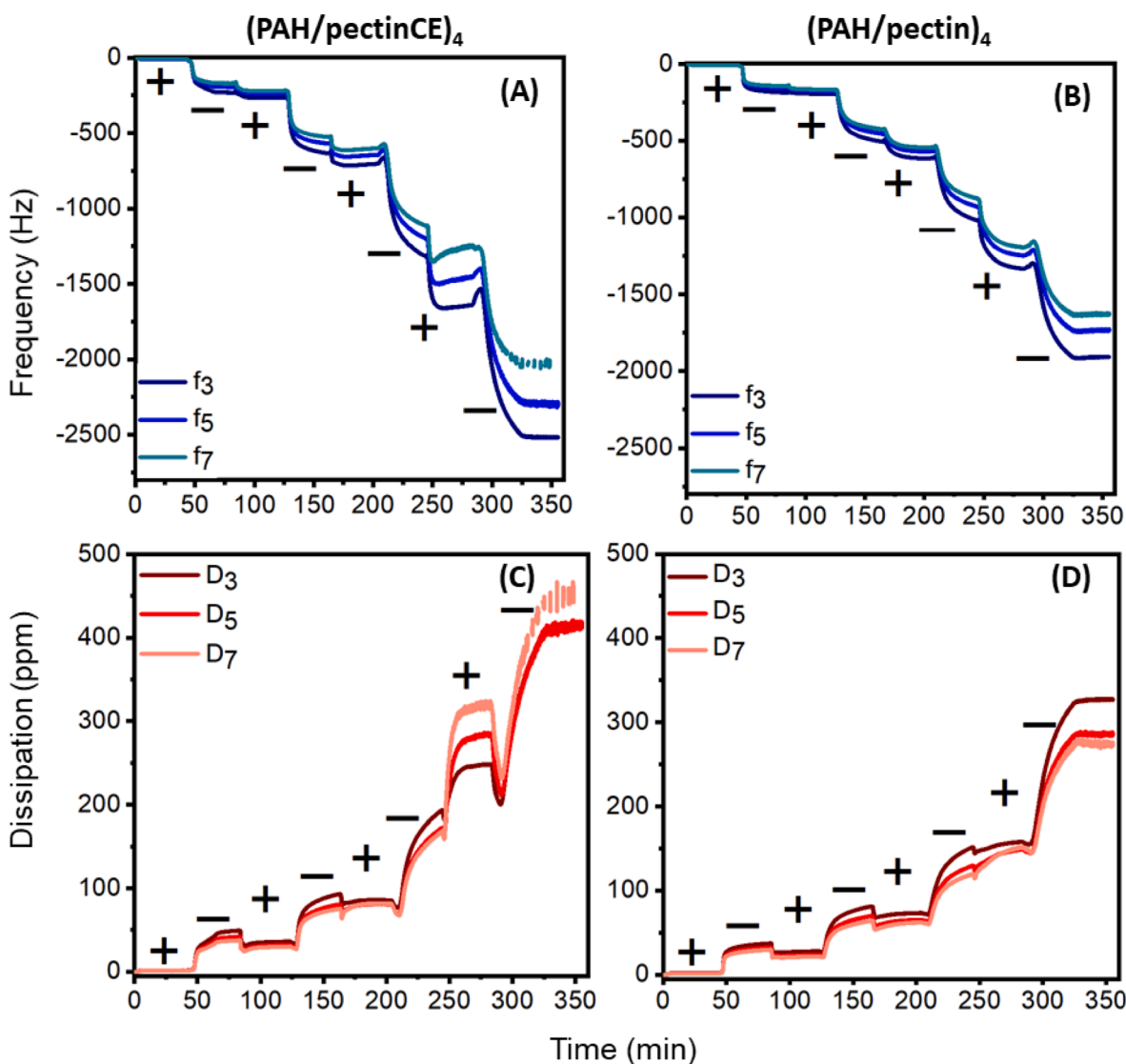


Fig. 4. Real-time QCM-D data showing representative changes in the frequency (A and B) and dissipation (C and D) for the 3rd, 5th, and 7th overtones of the build-up of (PAH/pectinCE)₄ and (PAH/pectin)₄ in 0.15 M CsCl. The plus and minus signs represent the polycation and polyanion in the PEMs, respectively.

mainly originating from the polyanion (pectin or pectinCE) layers, which is in line with the few reported QCM studies using pectin [81,82].

Using pectin instead of PSS resulted not only in higher overall shifts, but also affected the PEM build-up in at least the following two ways. First, coating steps that involve pectin(CE) show longer stabilization times compared to PSS (30 vs. 10 min per layer). Second, while the PAH(CE)/PSS system shows an almost linear frequency change during the PEM build-up, the PAH/pectin(CE) system shows a non-uniform growth pattern, where changes in f and D increase during the PEM build-up. In more detail, the overtones overlap more in the beginning of the process and the PEM eventually becomes more viscoelastic. It becomes clear from the growth patterns that pectin-containing PEMs are larger in size and more heterogeneous compared to the ones with PSS (with or without CE units). The heterogeneity (e.g. more voids) in the structure of the PAH/pectin(CE) could explain the aforementioned non-linear growth pattern, as in such a system more PAH can move in the PEM and lead to further interpenetration of polyelectrolytes. This would cause a less neatly stacked PEM and therefore would increase the possibility of adsorption of larger amounts of pectin(CE).

Furthermore, the use of pectinCE instead of pectin resulted in a higher total frequency. This trend was also observed for PAH(CE)/PSS PEMs, but for pectin(CE) the increase is more pronounced (≈ 40 vs. $\approx 18\%$). Also, the dissipation value increases $\approx 50\%$ when using

pectinCE, while we observed hardly any dissipation effect of CE in the PAH(CE)/PSS system, as CE units possibly cause more voids in the PAH/pectin system.

Based on the above-described QCM-D data the thickness values of the (PAH/pectin(CE))₄ were modelled in a similar fashion with the (PAH(CE)/PSS)₄ via the Sauerbrey equation (Table 1, bottom entries). As expected based on its higher frequency shift, (PAH/pectin(CE))₄ resulted in a thickness that is $\approx 40\%$ higher than the one of (PAH/pectin)₄. Due to limitations of the modelling software (DFind), Voigt thicknesses could not be obtained for PAH/pectin(CE) as the data did not fit the modelling after a certain number of layers (≈ 6 th layer).

Finally, the optical thickness of air-dried PEMs were measured and found to be smaller than the wet thickness values, as expected. (PAH/pectin(CE))₄ was found to be ≈ 1.7 times thicker than (PAH/pectin)₄. Moreover, when compared to PAH(CE)/PSS PEMs, PAH/pectin(CE) PEMs were found to be thicker (Table 1, bottom entries). For instance, the Sauerbrey thickness of (PAH/pectin)₄ is ≈ 8 times larger than (PAH/PSS)₄, indicating the effect of different polyanion on PEM thickness. Also, the Sauerbrey thickness of (PAH/pectin(CE))₄ is ≈ 10 times larger than the one of (PAHCE/PSS)₄.

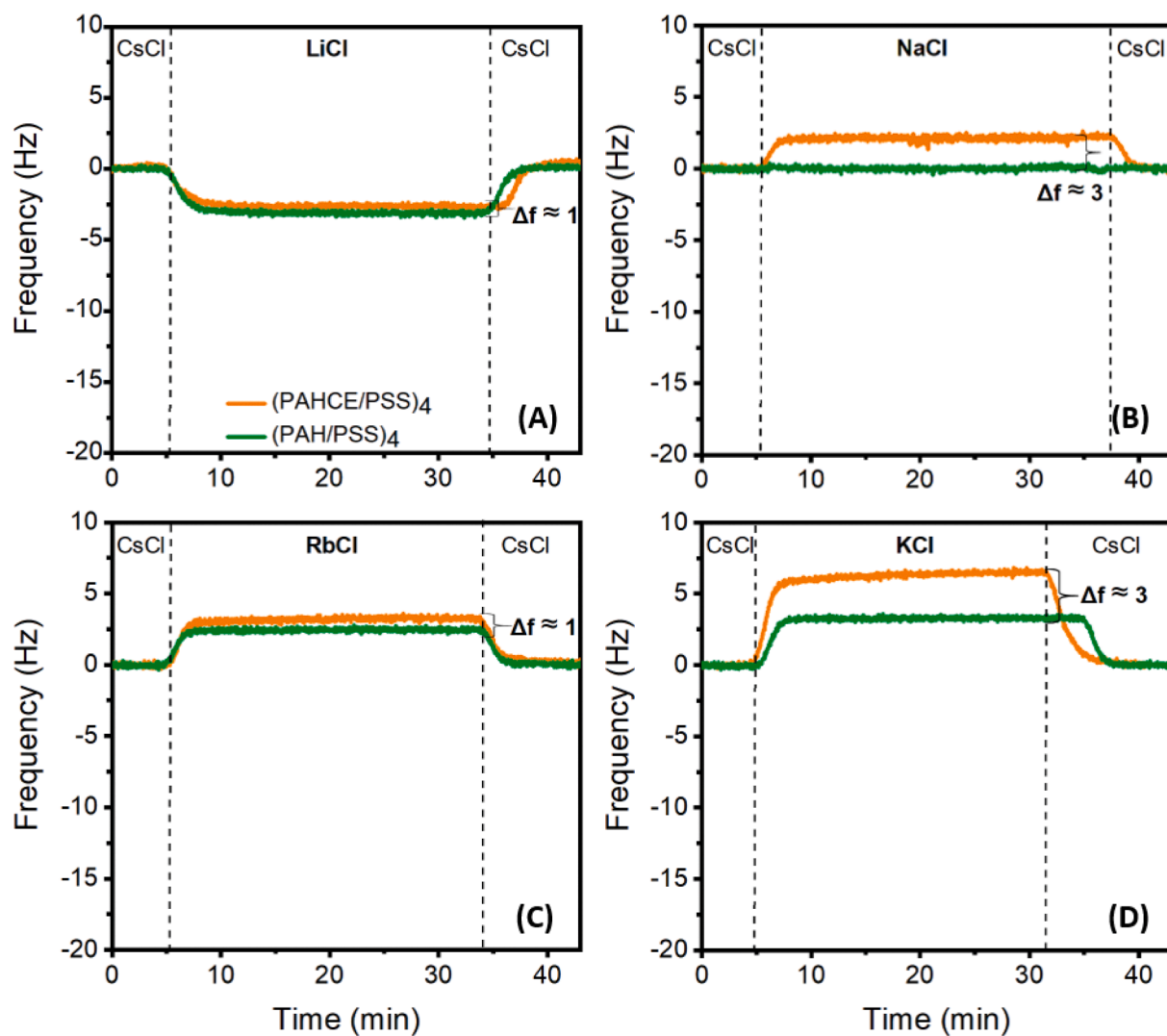


Fig. 5. Frequency change (3^{rd} harmonic) as a function of time, recorded for the QCM-D sensors coated with (PAHCE/PSS)₄ (orange), (PAH/PSS)₄ (green) exposed to cycle of changing the 0.15 M salt solution: from CsCl to XCl (where X is Li, Na, Rb or Cs), followed by a final rinsing step using CsCl. The dashed lines indicate the moment in time at which the salt solutions were switched.

3.4. Salt-exchange experiments with QCM-D

Since PEM properties are determined by the type of counterion and the ion concentration, PEMs are sensitive to post-assembly conditions [30,50]. Therefore, interactions between PEMs and various ions can be studied via salt-exchange experiments. This approach has been pursued for PEMs (without ionophore units) to study the post-assembly changes in PEMs by exposing them to solutions with different anions [58,59]. When a PEM is rinsed successively with solutions that each contain a different salt, ionic interactions can be understood based on the changes in frequency and dissipation. For this purpose, we performed a series of experiments and tested the effect of various parameters on cationic interactions of CE-containing and PEMs and their non-functionalized equivalents. In order to study whether PEMs with a crown ether show a preference towards a certain type of cation, CsCl was chosen as a supporting electrolyte during the build-up of all PEM coatings and also as the background electrolyte during all washing and stabilization steps.

3.4.1. Effect of crown ether units in (PAH/PSS)₄ PEMs

Fig. 5 presents the frequency shifts as a function of time recorded for both (PAH/PSS)₄ and (PAHCE/PSS)₄ before and after exposure to solutions containing 0.15 M of LiCl, NaCl, KCl, or RbCl. When switching from CsCl to another salt solution, a certain amount of Cs⁺ can be replaced by the other cation due to the concentration gradient (diffusion), as previously described for various QCM-D experiments where anion-exchange behavior of the PEMs was investigated [9,30,58]. Each salt was studied in a separate experiment and for all experiments the PEMs were rinsed with a CsCl solution before and after being exposed to the specified salt (indicated with dashed lines in Fig. 5).

Before investigating the effect of CE on the PEM-cation interactions, the interactions of (PAH/PSS)₄ with different salts were studied (indicated as green lines in Fig. 5). The shifts in frequency and dissipation were observed to be salt-dependent. A change in frequency can be explained by a combined effect of the *i*) difference in amount and weight of any cation exchange, and *ii*) difference in the amount of water that is associated to the PEM and/or counterion present in the PEM. Upon changing from Cs⁺ to Li⁺ the frequency decreased (Fig. 5A), indicated an increase in adsorbed mass. Considering the much smaller atomic mass of Li compared to Cs (6.94 amu vs. 132.91 amu), this difference can be attributed to the higher degree of hydration of Li⁺ (3.82 Å vs. 3.29 Å for Li⁺ and Cs⁺, respectively) [82] and/or the uptake of more Li⁺. On the other hand, when switching from Cs⁺ to K⁺ or Rb⁺ (Fig. 5C and D) an increase in frequency is observed, suggesting a decrease in mass. Considering that the hydrated sizes of Rb⁺ and Cs⁺ are comparable (~3.29 Å) [83] and the difference in atomic mass (132.91 amu vs. 85.47 amu for Cs and Rb, respectively), the difference in *f* can be rationalized by the difference in atomic mass of the cation itself. Similarly, K⁺ has a smaller atomic mass (39.10 amu) than Cs⁺, but their hydrated sizes are comparable (3.31 Å vs. 3.29 Å, for K⁺ and Cs⁺, respectively) [83], indicating that the increase in frequency (*i.e.* lower mass) can be explained by the smaller atomic mass of K⁺ compared to Cs⁺. Lastly, when switching to Na⁺ (3.58 Å, [83] 22.99 amu) the difference in atomic weight and hydrated size of Na⁺ and Cs⁺ balance each other and no significant change in frequency was observed. Trend-wise our observations are in line with studies where anion-exchange properties of PEMs were studied [28,33,61]. In these studies, increased changes in frequency were observed when PEMs were exposed to solutions with anions with higher atomic mass and/or hydrated size.

Next we discuss the changes in QCM-D data for the (PAHCE/PSS)₄ system. The orange-colored graphs in Fig. 5 represent the frequency changes for (PAHCE/PSS)₄ for different salt solutions. While the changes in frequency for Li⁺ and Rb⁺ are within ≈1 Hz, the difference for K⁺ and Na⁺ due to the presence of CE units is larger (3 Hz). Qualitatively, these results are in line with literature reporting on the use of 15-crown-5 in membrane-based electro dialysis [4] and nanofiltration [10] processes. Furthermore, the selectivity of CE units for both Na⁺ and K⁺ has also

been studied theoretically [84]

After comparing (PAHCE/PSS)₄ with (PAH/PSS)₄ for monovalent cations, 0.15 M CsCl solution was replaced with 0.15 M MgCl₂ solution to study the effect of a divalent cation. Fig. 6 shows a change in frequency of ≈15 Hz when changing the salt solutions from CsCl to MgCl₂ to CsCl, indicating an increased mass. As the atomic mass of Mg is smaller than the one of Cs (24.31 amu vs. 132.91 amu), the difference originated from differences in the amount of hydration. The hydrated size of Mg²⁺ is larger than the one of Cs (4.28 Å vs. 3.29 Å) [83]. A comparable effect was also observed in literature where a monovalent anion, Cl⁻, was replaced by divalent anions, SO₄²⁻ and HPO₄²⁻ [60]. As the difference between the two PEM systems for Mg²⁺ was found to be ≈1 Hz, similar to the results of Li⁺ and Rb⁺, the QCM data indicates that the presence of CE units does not affect the affinity to Mg²⁺. It is noted that the overall frequency change, *i.e.*, after switching back to CsCl, is about -2 Hz, but at the same time the frequency signal seemed to have drifted with a comparable value during the exposure of the PEM to MgCl₂.

All frequency and dissipation data for the aforementioned experiments were combined in Figs. S15 and S16 in ESI. The dissipation data supports the trends observed in frequency trends. In other words, when there is a decrease in frequency, an increase in dissipation is observed. Also, cations with a relatively larger hydrated size cause a larger increase in dissipation.

3.4.2. Effect of type of terminating layer

In addition to the effect of CE units, we studied the effect of the type of terminating layer on the salt-exchange behavior of the PEMs. For this purpose, (PAHCE/PSS)_{3,5} was coated on gold QCM sensors. Fig. S17 demonstrates the change in frequency and dissipation shifts for the build-up of (PAHCE/PSS)_{3,5} where the outermost layer is PAHCE. The trends in frequency and dissipation are in line with our observations for (PAHCE/PSS)₄, just like those of the modelled data and optical thickness (Table 1).

After the (PAHCE/PSS)_{3,5} PEM was built-up in a 0.15 M CsCl solution, salt-exchange experiments with LiCl, NaCl, and KCl were conducted. Fig. 7 shows the change in frequency in time for (PAHCE/PSS)_{3,5} before and after exposure to different salt solutions. Unlike the trends observed for PAHCE-terminated PEM, obtaining a stable signal takes

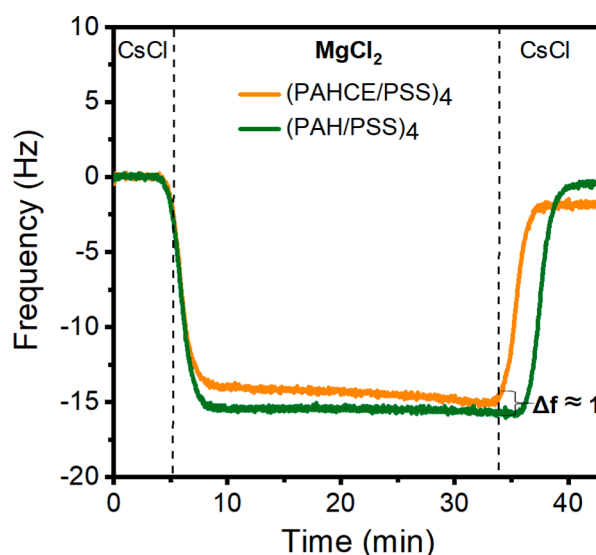


Fig. 6. Frequency change (3rd harmonic) as a function of time, recorded for the QCM-D sensors coated with (PAH/PSS)₄ (orange), (PAH/PSS)₄ (green) exposed to cycle of changing the 0.15 M salt solution: from CsCl to MgCl₂, followed by a final rinsing step using CsCl. The dashed lines indicate the moment in time at which the salt solutions were switched.

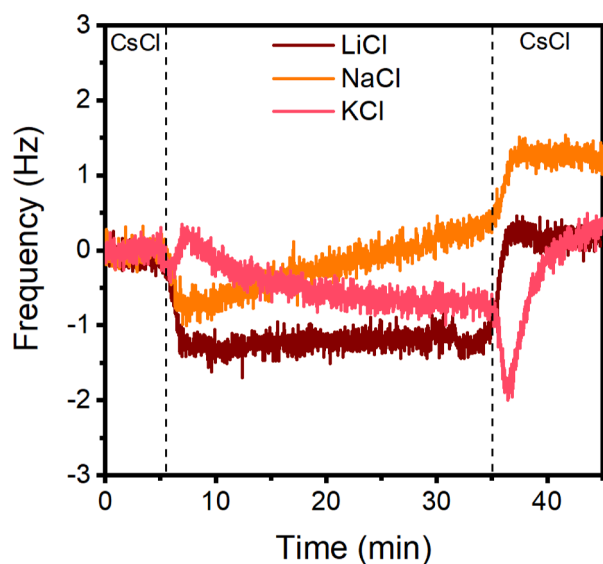


Fig. 7. Frequency change (3^{rd} harmonic) as a function of time, recorded for the QCM-D sensors coated with (PAHCE/PSS) $_4$ (orange), (PAH/PSS) $_4$ (green) exposed to cycle of changing the 0.15 M salt solution: from CsCl to XCl (where X is Li, Na, or K), followed by a final rinsing step using CsCl. The dashed lines indicate the moment in time at which the salt solutions were switched.

longer or it is not obtained at all. Also, the overall changes are clearly smaller than the ones for PSS-terminated PEM (Table S1, ESI), further confirming that the PSS-terminated PEM provides a better stability and increased salt-exchange. These differences can be explained by the rejection between the positively-charged terminating layer and the cations, a phenomenon that also has been described in, e.g., PEM-assisted electrodialysis processes [16,85].

3.4.3. Effect of PEM structure on salt-exchange

Next, the salt-exchange experiments were performed for the two different PEM structures. For this purpose, (PAH/pectin) $_4$ and (PAH/pectinCE) $_4$ were exposed to LiCl, NaCl, and KCl solutions and the resulting QCM transients are shown in Fig. 8. The green lines represent (PAH/pectin) $_4$ and when the CsCl solution is replaced by solutions containing other salts, the frequency values increase, i.e. 12.8 ± 1.8 , 10.5 ± 1.0 , and 14.0 ± 1.6 Hz for Li $^+$, Na $^+$, and K $^+$, respectively. The absolute values of these changes are larger than those of the (PAH/PSS) $_4$ (-0.3 ± 0.7 , -0.4 ± 0.7 , and 3.3 ± 0.5 Hz for Li $^+$, Na $^+$, and K $^+$, respectively), due to the bigger size of the (PAH/pectin) $_4$ multilayer. It should be realized that they are roughly the same for all three cations (12 ± 3 Hz).

When CE units are introduced to (PAH/pectin) $_4$, the difference in frequency shifts was found to be ≈ 1 Hz for after switching to a LiCl solution, a result that is similar to what was observed for the (PAH(CE)/PSS) $_4$ PEMs. Just like in the case of (PAHCE/PSS) $_4$, both Na $^+$ and K $^+$ result in a larger frequency, 6 and 12 Hz, respectively), which can again be related to the preferred interaction with the CE. These values are a factor of 2 to 4 higher than the ones observed for (PAHCE/PSS) $_4$, i.e., 3 Hz for both Na $^+$ and K $^+$. This may be related to the position of the CE units as for the (PAH/pectinCE) $_4$ system these are attached to the terminating layers, making them in direct contact with the solution. Additionally, the larger heterogeneity of the layers in PAH/pectinCE, and therefore the increase in pectinCE adsorption, can contribute to a higher number of CE units in the PEM, resulting in higher frequency values during the salt-exchange experiments.

4. Conclusions

This study describes the effect of a fossil- and a bio-based

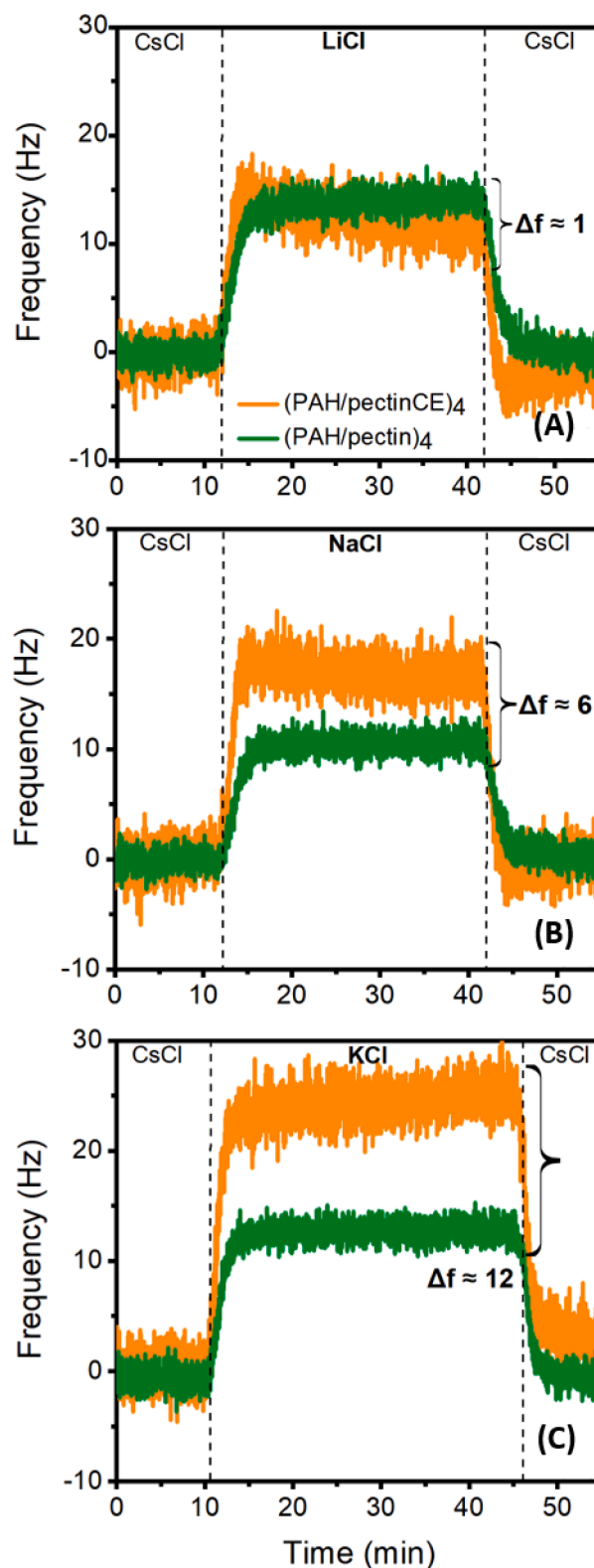


Fig. 8. Frequency change (3^{rd} harmonic) as a function of time, recorded for the QCM-D sensors coated with (PAH/pectinCE) $_4$ (orange), (PAH/pectin) $_4$ (green) exposed to cycle of changing the 0.15 M salt solution: from CsCl to XCl (where X is Li, Na, or K), followed by a final rinsing step using CsCl. The dashed lines indicate the moment in time at which the salt solutions were switched.

polyelectrolyte – to which a crown ether, 15-crown-5, was covalently attached – on the structural properties of PEMs. These properties were monitored real-time with QCM-D, both during the PEM build-up and afterwards when exposed to different salt solutions with a strong focus on alkali metal ionic and valency effects several cations. QCM-related frequency changes were rationalized by the differences in the molecular mass of the modified and non-modified PE building blocks and the mass and hydration properties of cations. Additionally, changes in the dissipation were related to the density of the PEM and hydration size of the cation present in the solution. The presence of crown ether units in the PEM was found to result in an increased (wet and dry) thickness, higher swelling degree and an increased preference towards Na^+ and K^+ . This shows that the cation-exchange behavior of PEMs can be increased via the introduction of covalently attached crown ethers. Moreover, this behavior also depends on which layer ‘lies on top’ in the PEM, and varies substantially for mono- and divalent cations. Considering the large amount of possible combinations of fossil- and/or bio-based polyelectrolytes with various ionophores, tailor-made, stable, ion-selective PEM coatings can likely be made for different desalination and medical applications, where ion selectivity is the crucial part of the separation or detection. Such work, which is of special importance for the recovery and sensing of specific ions, is currently ongoing in our laboratories.

Associated content

Supporting Information includes additional NMR spectra of the reactants, PAHCE, and pectinCE, FT-IR of pectinCE, XPS spectra of the bare and pectinCE-modified gold substrates, additional data for the salt exchange experiments with $(\text{PAH}(\text{CE})/\text{PSS})_4$ and $(\text{PAH}/\text{pectin}(\text{CE}))_4$, and real-time change in frequency and dissipation shifts for the build-up of $(\text{PAHCE}/\text{PSS})_{3,5}$, the overview of frequency and dissipation shifts during the salt exchange experiments with $(\text{PAHCE}/\text{PSS})_{3,5}$, as well as the a table with specifications of the three PEs used in this study.

Author contributions

S.S. wrote first draft and all the other authors gave input for the manuscript.

Funding sources

This study was supported by the European Research Council (ERC Consolidator Grant 682444, E-motion, PI de Smet).

Declaration of Competing Interest

All authors are aware of the submission and agree to its publication. The authors declare no conflict of interest.

Acknowledgment

The authors thank Nathalja Berghuis (formerly working at Wageningen University) for performing initial studies on combing crown ethers with polyelectrolytes. Lucas Teunissen and Barend van Lagen (both Wageningen University) are thanked for ellipsometry analyses and XPS measurements, respectively.

Supplementary materials

Supplementary material associated with this article can be found, in the online version, at doi:10.1016/j.apsadv.2022.100271.

References

- [1] Z. Zhang, Q. Dou, H. Gao, B. Bai, Y. Zhang, D. Hu, A.K. Yetisen, H. Butt, X. Yang, C. Li, Q. Dai, 30 s response time of K^+ ion-selective hydrogels functionalized with 18-crown-6 ether based on QCM sensor, *Adv. Healthc. Mater.* 7 (2018), 1700873, <https://doi.org/10.1002/adhm.201700873>.
- [2] Z. Cao, J. Guo, X. Fan, J. Xu, Z. Fan, B. Du, Detection of heavy metal ions in aqueous solution by P(MBTVBC-co-VIM)-coated QCM sensor, *Sens. Actuators B Chem.* 157 (2011) 34–41, <https://doi.org/10.1016/j.snb.2011.03.023>.
- [3] S. Sahin, J.E. Dykstra, H. Zuillhof, R.L. Zornitta, L.C.P.M. De Smet, Modification of cation-exchange membranes with polyelectrolyte multilayers to tune ion selectivity in capacitive deionization, *ACS Appl. Mater. Interfaces* 12 (2020) 34746–34754, <https://doi.org/10.1021/acsami.0c05664>.
- [4] Z. Qian, H. Miedema, S. Sahin, L.C.P.M. de Smet, E.J.R. Sudhölter, Separation of alkali metal cations by a supported liquid membrane (SLM) operating under electro dialysis (ED) conditions, *Desalination* 495 (2020) 114631, <https://doi.org/10.1016/j.desal.2020.114631>.
- [5] K. Singh, S. Sahin, J.G. Gamaethiralalage, R.L. Zornitta, L.C.P.M. de Smet, Simultaneous, monovalent ion selectivity with polyelectrolyte multilayers and intercalation electrodes in capacitive deionization, *Chem. Eng. J.* (2021), 128329, <https://doi.org/10.1016/j.cej.2020.128329>.
- [6] L. Paltrinieri, M. Wang, S. Sachdeva, N.A.M. Besseling, E.J.R. Sudhölter, L.C.P.M. de Smet, Fe_3O_4 nanoparticles coated with a guanidinium-functionalized polyelectrolyte extend the pH range for phosphate binding, *J. Mater. Chem. A* 5 (2017) 18476–18485, <https://doi.org/10.1039/c7ta04054g>.
- [7] A. Birukov, N. Rakova, K. Lerchl, R.H.G. Olde Engberink, B. Johannes, P. Wabel, U. Moissl, M. Rauh, F.C. Luft, J. Titz, Ultra-long-term human salt balance studies reveal interrelations between sodium, potassium, and chloride intake and excretion, *Am. J. Clin. Nutr.* 104 (2016) 49–57, <https://doi.org/10.3945/ajcn.116.132951>.
- [8] L. Paltrinieri, K. Remmen, B. Müller, L. Chu, J. Köser, T. Wintgens, M. Wessling, L.C.P.M. de Smet, E.J.R. Sudhölter, Improved phosphoric acid recovery from sewage sludge ash using layer-by-layer modified membranes, *J. Memb. Sci.* 587 (2019), 117162, <https://doi.org/10.1016/j.memsci.2019.06.002>.
- [9] Z. Cao, P.I. Gordichuk, K. Loos, E.J.R. Sudhölter, L.C.P.M. de Smet, The effect of guanidinium functionalization on the structural properties and anion affinity of polyelectrolyte multilayers, *Soft Matter* 12 (2016) 1496–1505, <https://doi.org/10.1039/c5sm01655j>.
- [10] M. Kazemabad, A. Verliefe, E.R. Cornelissen, A. D’Haese, Crown ether containing polyelectrolyte multilayer membranes for lithium recovery, *J. Memb. Sci.* 595 (2020), 117432, <https://doi.org/10.1016/j.memsci.2019.117432>.
- [11] J.G. Gamaethiralalage, K. Singh, S. Sahin, J. Yoon, M. Elimelech, M.E. Suss, P. Liang, P.M. Biesheuvel, R.L. Zornitta, L.C.P.M. de Smet, Recent advances in ion selectivity with capacitive deionization, *Energy Environ. Sci.* 14 (2020) 1095–1120, <https://doi.org/10.1039/d0ee03145c>.
- [12] A. Jose, J.G. Ray, Toxic heavy metals in human blood in relation to certain food and environmental samples in Kerala, South India, *Environ. Sci. Pollut. Res.* 25 (2018) 7946–7953, <https://doi.org/10.1007/s11356-017-1112-x>.
- [13] S. Sahin, J.E. Dykstra, H. Zuillhof, R.L. Zornitta, L.C.P.M. de Smet, Modification of cation-exchange membranes with polyelectrolyte multilayers to tune ion selectivity in capacitive deionization, *ACS Appl. Mater. Interfaces* 12 (2020) 34746–34754, <https://doi.org/10.1021/acsami.0c05664>.
- [14] N. White, M. Misovich, A. Yaroshchuk, M.L. Bruening, Coating of nafion membranes with polyelectrolyte multilayers to achieve high monovalent/divalent cation electro dialysis selectivities, *ACS Appl. Mater. Interfaces* 7 (2015) 6620–6628, <https://doi.org/10.1021/am508945p>.
- [15] M. Ahmad, C. Tang, L. Yang, A. Yaroshchuk, M.L. Bruening, Layer-by-layer modification of aliphatic polyamide anion-exchange membranes to increase $\text{Cl}^-/\text{SO}_4^{2-}$ selectivity, *J. Memb. Sci.* 578 (2019) 209–219, <https://doi.org/10.1016/j.memsci.2019.02.018>.
- [16] S. Mulyati, R. Takagi, A. Fujii, Y. Ohmukai, H. Matsuyama, Simultaneous improvement of the monovalent anion selectivity and antifouling properties of an anion exchange membrane in an electro dialysis process, using polyelectrolyte multilayer deposition, *J. Memb. Sci.* 431 (2013) 113–120, <https://doi.org/10.1016/j.memsci.2012.12.022>.
- [17] J.J. Richardson, M. Björnmalm, F. Caruso, Technology-driven layer-by-layer assembly of nanofilms, *Science* (2015) 348, <https://doi.org/10.1126/science.aaa2491>.
- [18] J.J. Richardson, J. Cui, M. Björnmalm, J.A. Braunger, H. Ejima, F. Caruso, Innovation in layer-by-layer assembly, *Chem. Rev.* 116 (2016) 14828–14867, <https://doi.org/10.1021/acs.chemrev.6b00627>.
- [19] F. Caruso, K. Niikura, D.N. Furlong, Y. Okahata, I. Ultrathin multilayer polyelectrolyte films on gold: Construction and thickness determination, *Langmuir* 13 (1997) 3422–3426, <https://doi.org/10.1021/la960821a>.
- [20] J. Movilli, J. Huskens, Functionalized polyelectrolytes for bioengineered interfaces and biosensing applications, *Org. Mater.* 02 (2020) 078–107, <https://doi.org/10.1055/s-0040-1708494>.
- [21] T. Zahn, R. Voros, J. Zambelli, Tuning the electrochemical swelling of polyelectrolyte multilayers toward nanoactuation, *Langmuir* 30 (2014) 12057–12066, <https://doi.org/10.1021/la503051n>.
- [22] N. Joseph, P. Ahmadiannamini, R. Hoogenboom, I.F.J. Vankelecom, Layer-by-layer preparation of polyelectrolyte multilayer membranes for separation, *Polym. Chem.* 5 (2014) 1817–1831, <https://doi.org/10.1039/c3py01262j>.
- [23] X. Li, C. Liu, B. van der Bruggen, Polyelectrolytes self-assembly: versatile membrane fabrication strategy, *J. Mater. Chem. A* 8 (2020) 20870–20896, <https://doi.org/10.1039/d0ta07154d>.

- [24] D. Büttergerds, C. Kateloe, C. Cramer, M. Schönhoff, Influence of the degree of ionization on the growth mechanism of poly(diallyldimethylammonium)/poly (acrylic acid) multilayers, *J. Polym. Sci. Part B Polym. Phys.* 55 (2017) 425–434, <https://doi.org/10.1002/polb.24283>.
- [25] H. Riegler, F. Essler, Polyelectrolytes. 2: intrinsic or extrinsic charge compensation? Quantitative charge analysis of PAH/PSS multilayers, *Langmuir* 18 (2002) 6694–6698, <https://doi.org/10.1021/la020108n>.
- [26] H.M. Fares, J.B. Schlenoff, Equilibrium overcompensation in polyelectrolyte complexes, *Macromolecules* 50 (2017) 3968–3978, <https://doi.org/10.1021/acs.macromol.7b00665>.
- [27] K. Tang, N.A.M. Besseling, Formation of polyelectrolyte multilayers: ionic strengths and growth regimes, *Soft. Matter* 12 (2016) 1032–1040, <https://doi.org/10.1039/c5sm02118a>.
- [28] S.T. Dubas, J.B. Schlenoff, Factors controlling the growth of polyelectrolyte multilayers, *Macromolecules* 32 (1999) 8153–8160, <https://doi.org/10.1021/ma981927a>.
- [29] M. Lösche, J. Schmitt, G. Decher, W.G. Bouwman, K. Kjaer, Detailed structure of molecularly thin polyelectrolyte multilayer films on solid substrates as revealed by neutron reflectometry, *Macromolecules* 31 (1998) 8893–8906, <https://doi.org/10.1021/ma980910p>.
- [30] M. Salomäki, T. Laiho, J. Kankare, Counteranion-controlled properties of polyelectrolyte multilayers, *Macromolecules* 37 (2004) 9585–9590, <https://doi.org/10.1021/ma048701u>.
- [31] M. Salomäki, J. Kankare, Specific anion effect in swelling of polyelectrolyte multilayers, *Macromolecules* 41 (2008) 4423–4428, <https://doi.org/10.1021/ma800315j>.
- [32] A.E. El Haitami, D. Martel, V. Ball, H.C. Nguyen, E. Gonthier, P. Labbe, J.C. Voegel, P. Schaaf, B. Senger, F. Boulmedais, Effect of the supporting electrolyte anion on the thickness of PSS/PAH multilayer films and on their permeability to an electroactive probe, *Langmuir* 25 (2009) 2282–2289, <https://doi.org/10.1021/la803534y>.
- [33] M. Salomäki, P. Tervasmäki, S. Areva, J. Kankare, The Hofmeister anion effect and the growth of polyelectrolyte multilayers, *Langmuir* 20 (2004) 3679–3683, <https://doi.org/10.1021/la036328y>.
- [34] M. Schönhoff, P. Bieker, Linear and exponential growth regimes of multilayers of weak polyelectrolytes in dependence on pH, *Macromolecules* 43 (2010) 5052–5059, <https://doi.org/10.1021/ma1007489>.
- [35] J.L. Vidyasaagar, A. C. Sung, K. Losensky, Lutkenshaus, pH-Dependent thermal transitions in hydrated layer-by-layer assemblies containing weak polyelectrolytes, *Macromol. Res.* 45 (2012) 9169–9176, <https://doi.org/10.1021/ma3020454>.
- [36] M. Ahmad, A. Yaroshchuk, M.L. Bruening, Moderate pH changes alter the fluxes, selectivities and limiting currents in ion transport through polyelectrolyte multilayers deposited on membranes, *J. Memb. Sci.* 616 (2020), 118570, <https://doi.org/10.1016/j.memsci.2020.118570>.
- [37] D. Yoo, S.S. Shiratori, M.F. Rubner, Controlling bilayer composition and surface wettability of sequentially adsorbed multilayers of weak polyelectrolytes, *Macromolecules* 31 (1998) 4309–4318, <https://doi.org/10.1021/ma9800360>.
- [38] T. Rijnaarts, D.M. Reurink, F. Radmanesh, W.M. de Vos, K. Nijmeijer, Layer-by-layer coatings on ion exchange membranes: Effect of multilayer charge and hydration on monovalent ion selectivities, *J. Memb. Sci.* 570–571 (2019) 513–521, <https://doi.org/10.1016/j.memsci.2018.10.074>.
- [39] A. Toutianoush, J. Schnepf, A. El Hashani, B. Tieke, Selective ion transport and complexation in layer-by-layer assemblies of p-sulfonato-calix[n] arenes and cationic polyelectrolytes, *Adv. Funct. Mater.* 15 (2005) 700–708, <https://doi.org/10.1002/adfm.200400223>.
- [40] H. Gu, R. Dai, Y. Wei, H.F. Ji, Functional layer-by-layer multilayer films for ion recognition, *Anal. Methods* 5 (2013) 3454–3457, <https://doi.org/10.1039/c3ay40372f>.
- [41] A.A. EV Stokolshchikova, A.V. Radaev, O.Y. Orlova, K.G. Nikolaev, Skorb, Thin and flexible ion sensors based on polyelectrolyte multilayers assembled onto the carbon adhesive tape, *ACS Omega* 4 (2019) 15421–15427, <https://doi.org/10.1021/acsomega.9b01464>.
- [42] L. Paltrinieri, E. Huerta, T. Puts, W. Van Baak, A.B. Verver, E.J.R. Sudhölter, L.C.P. M. de Smet, Functionalized anion-exchange membranes facilitate electro dialysis of citrate and phosphate from model dairy wastewater, *Environ. Sci. Technol.* 53 (2019) 2396–2404, <https://doi.org/10.1021/acs.est.8b05558>.
- [43] K.V. Petrov, L. Paltrinieri, L. Poltorak, L.C.P.M. de Smet, E.J.R. Sudho, Modified cation-exchange membrane for phosphate recovery in an electrochemically assisted adsorption–desorption process, *Chem. Commun.* 26 (2020) 5046–5049, <https://doi.org/10.1039/c9cc09563b>.
- [44] M.R. Awual, T. Yaita, T. Taguchi, H. Shiwaku, S. Suzuki, Y. Okamoto, Selective cesium removal from radioactive liquid waste by crown ether immobilized new class conjugate adsorbent, *J. Hazard. Mater.* 278 (2014) 227–235, <https://doi.org/10.1016/j.jhazmat.2014.06.011>.
- [45] J. Guo, J. Lee, C.I. Contescu, N.C. Gallego, S.T. Pantelides, S.J. Pennycook, B. A. Moyer, M.F. Chisholm, Crown ethers in graphene, *Nat. Commun.* 5 (2014) 1–6, <https://doi.org/10.1038/ncomms3689>.
- [46] O. Özbek, Ö. Isildak, M.B. Gürdere, A. Cetin, The use of crown ethers as sensor material in potentiometry technique, *Org. Commun.* (2021) 228–239, <https://doi.org/10.25135/acg.oc.110.2106.2114>.
- [47] R.V. Klitzing, B. Tieke, Polyelectrolyte membranes, *Adv. Polym. Sci.* (2004) 177–210, <https://doi.org/10.1007/b11270>.
- [48] L. Krasemann, B. Tieke, Selective ion transport across self-assembled alternating multilayers of cationic and anionic polyelectrolytes, *Langmuir* 16 (2000) 287–290, <https://doi.org/10.1021/la991240z>.
- [49] T. Huang, M. Alyami, N.M. Kashab, S.P. Nunes, Engineering membranes with macrocycles for precise molecular separations, *J. Mater. Chem. A* 9 (2021) 18102–18128, <https://doi.org/10.1039/d1ta02982g>.
- [50] M. O’Neal, J.T. Dai, E.Y. Zhang, Y. Clark, K.B. Wilcox, K.G. George, I. M. Ramasamy, N.E. Enriquez, D. Batys, P. Sannakkorpi, QCM-D investigation of swelling behavior of layer-by-layer thin films upon exposure to monovalent ions, *Langmuir* 34 (2018) 999–1009, <https://doi.org/10.1021/acs.langmuir.7b02836>.
- [51] Z. Feldötö, I. Varga, E. Blomberg, Influence of salt and rinsing protocol on the structure of PAH/PSS polyelectrolyte multilayers, *Langmuir* 26 (2010) 17048–17057, <https://doi.org/10.1021/la102351f>.
- [52] J. Wei, D.A. Hoagland, G. Zhang, Z. Su, Effect of divalent counterions on polyelectrolyte multilayer properties, *Macromolecules* 49 (2016) 1790–1797, <https://doi.org/10.1021/acs.macromol.5b02151>.
- [53] Z. Cao, Y. Zhang, Z. Luo, W. Li, T. Fu, W. Qiu, Z. Lai, J. Cheng, H. Yang, W. Ma, C. Liu, L.C.P.M. de Smet, Construction of a self-assembled polyelectrolyte/graphene oxide multilayer film and its interaction with metal ions, *Langmuir* 37 (2021) 12148–12162, <https://doi.org/10.1021/acs.langmuir.1c02058>.
- [54] X. Qiao, X. Zhang, Y. Tian, Y. Meng, Progresses on the theory and application of quartz crystal microbalance, *Appl. Phys. Rev.* 3 (2016), <https://doi.org/10.1063/1.4963312>.
- [55] M.C. Dixon, Quartz crystal microbalance with dissipation monitoring: enabling real-time characterization of biological materials and their interactions, *J. Biomol. Tech.* 19 (2008) 151–158.
- [56] G. Sauerbrey, Verwendung von schwingquarzen zur wägung dünner schichten und zur mikrowägung, *Z. Phys.* 155 (1959) 206–222, <https://doi.org/10.1007/BF01337937>.
- [57] N. Parveen, P.K. Jana, M. Schönhoff, Viscoelastic properties of polyelectrolyte multilayers swollen with ionic liquid solutions, *Polymers* 11 (2019), <https://doi.org/10.3390/polym11081285>.
- [58] R. Zahn, F. Boulmedais, J. Vörös, P. Schaaf, T. Zambelli, Ion and solvent exchange processes in PGA/PAH polyelectrolyte multilayers containing ferrocyanide, *J. Phys. Chem. B* 114 (2010) 3759–3768, <https://doi.org/10.1021/jp9106074>.
- [59] L. Wang, Y. Lin, Z. Su, Counterion exchange at the surface of polyelectrolyte multilayer film for wettability modulation, *Soft Matter* 5 (2009) 2072–2078, <https://doi.org/10.1039/b900638a>.
- [60] W.J. Dressick, K.J. Wahl, N.D. Bassim, R.M. Stroud, D.Y. Petrovykh, Divalent-anion salt effects in polyelectrolyte multilayer depositions, *Langmuir* 28 (2012) 15831–15843, <https://doi.org/10.1021/la3033176>.
- [61] G. Liu, Y. Hou, X. Xiao, G. Zhang, Specific anion effects on the growth of a polyelectrolyte multilayer in single and mixed electrolyte solutions investigated with quartz crystal microbalance, *J. Phys. Chem. B* 114 (2010) 9987–9993, <https://doi.org/10.1021/jp101826j>.
- [62] N. Chopin, X. Guillory, P. Weiss, J. Bideau, S. Collic-Jouault, Design polysaccharides of marine origin: chemical modifications to reach advanced versatile compounds, *Curr. Org. Chem.* 18 (2014) 867–895, <https://doi.org/10.2174/138527281807140515152334>.
- [63] S. Ding, X. Zhang, X. Feng, Y. Wang, S. Ma, Q. Peng, W. Zhang, Synthesis of N,N'-diallyl dibenzo 18-crown-6 crown ether crosslinked chitosan and their adsorption properties for metal ions, *React. Funct. Polym.* 66 (2006) 357–363, <https://doi.org/10.1016/j.reactfunctpolym.2005.08.008>.
- [64] A.A. Radwan, F.K. Alanazi, I.A. Alsarar, Microwave irradiation-assisted synthesis of a novel crown ether crosslinked chitosan as a chelating agent for heavy metal ions (M²⁺), *Molecules* 15 (2010) 6257–6268, <https://doi.org/10.3390/molecules15096257>.
- [65] X. Zhang, S. Ding, Y. Wang, X. Feng, Q. Peng, S. Ma, Synthesis and adsorption properties of metal ions of novel azacrown ether crosslinked chitosan, (2006) 2–6. 10.1002/app.22941.
- [66] C. Peng, Y. Wang, Y. Tang, Synthesis of crosslinked chitosan-crown ethers and evaluation of these products as adsorbents for metal ions, *J. Appl. Polym. Sci.* (1998) 501–506, [https://doi.org/10.1002/\(SICI\)1097-4628\(19981017\)70:3<501::AID-APP11>3.0.CO;2-3](https://doi.org/10.1002/(SICI)1097-4628(19981017)70:3<501::AID-APP11>3.0.CO;2-3).
- [67] X. Tang, S. Tan, Y. Wang, Study of the synthesis of chitosan derivatives containing benzo-21-crown-7 and their adsorption properties for metal ions, *J. Appl. Polym. Sci.* (2002) 1886–1891, <https://doi.org/10.1002/app.2316>.
- [68] L. Wan, Y. Wang, S. Qian, Study on the adsorption properties of novel crown ether crosslinked chitosan for metal ions, *J. Appl. Polym. Sci.* (2002) 29–34, <https://doi.org/10.1002/app.10180>.
- [69] C.J. Pedersen, Salts, cyclic polyethers and their complexes with metal salts, *J. Am. Chem. Soc.* 157 (1967) 7017–7036, <https://doi.org/10.1021/ja00986a052>.
- [70] R.C. D.J. Helgeson, K. Koga, J.M. Timko, Cram, structural requirements for cyclic ethers to complex and lipophilize metal cations or α -amino acids, *J. Am. Chem. Soc.* 95 (1973) 3023–3025.
- [71] R.M. Izatt, J.S. Bradshaw, S.A. Nielsen, J.D. Lamb, J.J. Christensen, D. Sen, Thermodynamic and kinetic data for cation-macrocycle interaction, *Chem. Rev.* 85 (1985) 271–339, <https://doi.org/10.1021/cr00068a003>.
- [72] S.Y. Lin, S.W. Liu, C.M. Lin, C.H. Chen, Recognition of potassium ion in water by 15-crown-5 functionalized gold nanoparticles, *Anal. Chem.* 74 (2002) 330–335, <https://doi.org/10.1021/ac015631p>.
- [73] H. Zhai, R. Qu, X. Li, Y. Liu, Y. Wei, L. Feng, Crown ether modified membranes for Na⁺-responsive controllable emulsion separation suitable for hypersaline environments, *J. Mater. Chem. A* 8 (2020) 2684–2690, <https://doi.org/10.1039/c9ta12418g>.
- [74] J. Moffat, T.R. Noel, R. Parker, N. Wellner, S.G. Ring, The environmental response and stability of pectin and poly-l-lysine multilayers, *Carbohydr. Polym.* 70 (2007) 422–429, <https://doi.org/10.1016/j.carbpol.2007.05.001>.

- [75] V. Ball, J.C. Voegel, P. Schaaf, Effect of thiocyanate counterion condensation on poly(allylamine hydrochloride) chains on the buildup and permeability of polystyrenesulfonate/polyallylamine polyelectrolyte multilayers, *Langmuir* 21 (2005) 4129–4137, <https://doi.org/10.1021/la047610n>.
- [76] M.E. Gokel, G.W. Leevy, W.M. Weber, Crown ethers: sensors for ions and molecular scaffolds for materials and biological models, *Chem. Rev.* 104 (2004) 2723–2750, <https://doi.org/10.1021/cr020080k>.
- [77] S.M. Notley, M. Eriksson, L. Wågberg, Visco-elastic and adhesive properties of adsorbed polyelectrolyte multilayers determined *in situ* with QCM-D and AFM measurements, *J. Colloid Interface Sci.* 292 (2005) 29–37, <https://doi.org/10.1016/j.jcis.2005.05.057>.
- [78] J.J. Iturri Ramos, S. Stahl, R.P. Richter, S.E. Moya, Water content and buildup of poly(diallyldimethylammonium chloride)/poly(sodium 4-styrenesulfonate) and poly(allylamine hydrochloride)/poly(sodium 4-styrenesulfonate) polyelectrolyte multilayers studied by an *in situ* combination of a quartz crystal microb, *Macromolecules* 43 (2010) 9063–9070, <https://doi.org/10.1021/ma1015984>.
- [79] I. Reviakine, D. Johannsmann, R.P. Richter, Hearing what you cannot see and visualizing what you hear: Interpreting quartz crystal microbalance data from solvated interfaces, *Anal. Chem.* 83 (2011) 8838–8848, <https://doi.org/10.1021/ac201778h>.
- [80] J. Kittle, J. Levin, N. Levin, Water content of polyelectrolyte multilayer films measured by quartz crystal microbalance and deuterium oxide exchange, *Sensors* 21 (2021) 1–12, <https://doi.org/10.3390/s21030771>.
- [81] L. Pastorino, S. Erokhina, C. Ruggiero, V. Erokhin, P. Petriani, Fabrication and characterization of chitosan and pectin nanostructured multilayers, *Macromol. Chem. Phys.* 216 (2015) 1067–1075, <https://doi.org/10.1002/macp.201400576>.
- [82] D. Lin, P. Lopez-Sanchez, N. Selway, M.J. Gidley, Viscoelastic properties of pectin/cellulose composites studied by QCM-D and oscillatory shear rheology, *Food Hydrocoll.* 79 (2018) 13–19, <https://doi.org/10.1016/j.foodhyd.2017.12.019>.
- [83] E.R. Nightingale, Phenomenological theory of ion solvation. Effective radii of hydrated ions, *J. Phys. Chem.* 63 (1959) 1381–1387, <https://doi.org/10.1021/j150579a011>.
- [84] S.E. Hill, D. Feller, Theoretical study of cation/ether complexes: 15-crown-5 and its alkali metal complexes, *Int. J. Mass Spectrom.* 201 (2000) 41–58, [https://doi.org/10.1016/S1387-3806\(00\)00214-1](https://doi.org/10.1016/S1387-3806(00)00214-1).
- [85] W. Cheng, C. Liu, T. Tong, R. Epsztein, M. Sun, R. Verduzco, J. Ma, M. Elimelech, Selective removal of divalent cations by polyelectrolyte multilayer nanofiltration membrane: role of polyelectrolyte charge, ion size, and ionic strength, *J. Memb. Sci.* 559 (2018) 98–106, <https://doi.org/10.1016/j.memsci.2018.04.052>.